Chapter 12
Turbulence Characteristics in a Rough Open Channel Under Unsteady Flow Conditions

Jnana Ranjan Khuntia, Kamalini Devi, Bhabani Shankar Das, and Kishanjit Kumar Khatua

Abstract The majority of open channel flows of interest to hydraulic engineers and hydrologists are unsteady. In unsteady flow cases, some aspects of flow (velocity, depth, viscosity, pressure, etc.) will be evolving in time. However, more numbers of issues identified with the unsteady flow have been roughly accepting as steady flow (for example, constant peak discharges in floodplains). Very few experimental investigations have been conveyed in previous literature to examine turbulence qualities in an open channel flow under unsteady flow states over rough beds. The present study investigates the vertical and horizontal fluctuating velocity profiles under unsteady flow states in a rectangular open channel. An experiment is conducted to observe the turbulence characteristics under unsteady flow conditions in a rough bed open channel for two different flow depths. One identical hydrograph is passed repeatedly through the rectangular flume with a fixed rough bed. The dense rough mat is used as a rough bed which replica of a dense grass bed. The flow patterns are investigated at both lateral and longitudinal positions over three different cross-sections by using a micro Pitot tube and Acoustic Doppler Velocimeter (ADV). For two given flow depths, the velocities on both the rising and falling limbs are observed and analyzed. Hysteresis effect loop between stage-discharge (h ~ Q) rating curve between the rising and falling limbs is illustrated. Turbulence characteristics, i. e., variations of lateral and vertical Reynolds stresses, are analyzed from measured fluctuation velocities.

J. R. Khuntia (✉)
Department of Civil Engineering, St. Martin's Engineering College, Dhulapally, Secunderabad, Telangana 500100, India

J. R. Khuntia · K. K. Khatua
Department of Civil Engineering, National Institute of Technology, Rourkela, Odisha 769008, India

K. Devi
Department of Civil Engineering, Vidya Jyothi Institute of Technology, Hyderabad, Telengana 500075, India

B. S. Das
Department of Civil Engineering, National Institute of Technology, Patna, Bihar 800005, India

R. Jha et al. (eds.), *River Hydraulics*, Water Science and Technology Library 110,
https://doi.org/10.1007/978-3-030-81768-8_12

Keywords Open channel flow · Unsteady flow · Rough bed · Hydrograph · Fluctuating velocity · Hysteresis loop · Reynolds stress

12.1 Introduction

Flows in the regular waterways, rivers, and channels are frequently unsteady. At the point when discharge changes gradually, the issue of unsteady flow can be comprehended with the state of steady flow (Mahmood and Yevjevich 1975). However, in some extraordinary cases, for example, reservoir activities, where discharge fluctuates quickly, the learning of steady flow may prompt unique or mistaken outcomes when managing issues of sediment transport, scour, deposition, etc. (Song and Graf 1996). So, the study of unsteady open channel flow has become an important issue for hydraulic engineering. An understanding of the mean velocity, bed shear stress, and turbulence characteristics under unsteady open channel flow conditions is needed, e.g., to predict the flood passage (hysteresis in the stage-discharge relationships between falling and rising limbs) and the river morphology processes dependent on unsteady effects. There are very few literatures found on the experimental investigation in unsteady flow over the rough bed. Tu and Graf (1992) used micro propellers to study the velocity distribution in unsteady open channel flow. They obtained the friction velocity as well as the shear stress distribution, but the turbulence was not measured.

Previous experimental research (Nezu et al. 1994a, b; Anwar and Atkins 1980; De Sutter et al. 2001; Ahanger et al. 2008; Bombar et al. 2011; Martin and Jerolmack 2013) investigated unsteady flow events in a laboratory fixed bank sand-bed channels using hydrographs of different shapes (e.g., trapezoidal, triangular, etc.) and varying characteristics. General conclusions from the literature suggest that few experimental works have been done in response to unsteady flow event hydrograph. Despite this research, to date, no systematic effort has been done for the shape of the unsteady flow event hydrograph over a fixed rough bed and their flow variables. De Sutter et al. (1970, 2001) and Hu et al. (2012) state that a dynamic hydrograph showed hysteresis effects. This means, for the same discharge value, a higher water height was obtained in the falling limb than the rising limb.

Velasco et al. (2003) considered the impact of turbulence on flow in an open channel utilizing plastic plants seeded in a gravel bed. Their outcomes uncovered that minimal value of friction factor is obtained for totally flexible plants under favorable conditions where the relative deflection of plant height was within the range of 0.4–0.5. Huai et al. (2012) investigated the flow characteristics of turbulent open channel flow with submerged vegetation. They experimented by separating the flow into three sections in vertical direction from bed to water surface level. The three layers are basal non-vegetated layer, inner vegetation layer, and upper vegetation layer. Suspended vegetation in open channels impedes flow, for which the longitudinal velocity distribution in vertical direction was deviated from the basic logarithmic law. Further, the Mixing length theory was implemented to find the boundary shear

stress in the internal and non-vegetation layers. Some hydraulic parameters were determined by using the data sets of Plew's laboratory measurements.

Dupuis et al. (2017) investigated the flow characteristics on longitudinal roughness changes of submerged dense rough bed and emerged rigid vegetation by using artificial dense plastic grass and wooden cylinders, respectively. Turbulence production and magnitude of secondary currents were increased by the presence of emergent rigid elements over the floodplains. The mixing layer development in longitudinal direction is also investigated for two stage open channel flow.

The main objective of the present study is to investigate the fluctuating velocities (i.e., u', v′ and w') and Reynolds stresses (i.e., $\overline{u'v'}$ or $\rho u'v'$,$\overline{v'w'}$ or $\rho v'w'$ and $\overline{u'w'}$ or $\rho u'w'$) by laboratory experimentation under unsteady flow conditions over the rough bed. Also, Reynolds stresses have been compared at a lower depth case as well as a higher depth case in both rising and falling limbs of a hydrograph.

12.2 Experimental Set-up and Procedures

The experiments were carried out in a 12 m long, 0.6 m wide and 0.6 m deep recirculating, rectangular, tilting flume in the Hydraulics Engineering Laboratory (H. E. Lab.) of Civil Engineering, National Institute of Technology Rourkela (Khuntia et al. 2018a, 2019). The flume has glass walls in the testing section and the rest walls and bottom are of mild steel. The bottom of flume has been modified as a rough bed by fixing rigid grass along the channel bed. A schematic diagram of the experimental set-up is shown in Fig. 12.1. Photographs of the experimental set-up, H. E. Lab., NITR are shown in Fig. 12.2. An electromagnetic flowmeter is fitted with an inlet pipe upstream to measure the flow discharges. Three-point gauges are fixed to measure the flow depth at different positions along the centre line of the flume. A longitudinal slope (S_0) of approximately 1.2 cm in 10 m was considered and kept unchanged throughout the experimental program.

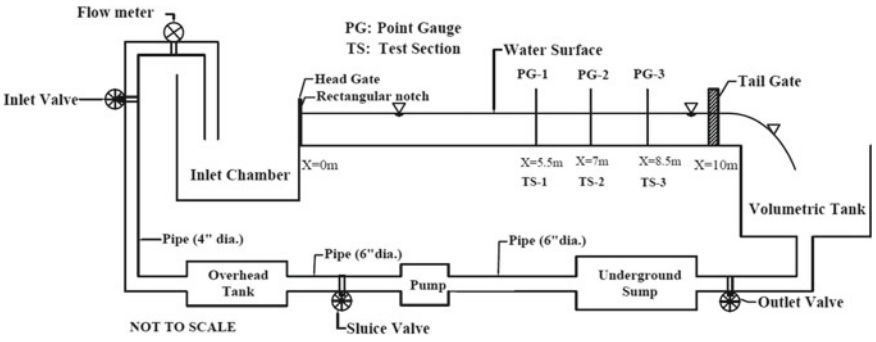

Fig. 12.1 A schematic diagram of the experimental set-up, NITR

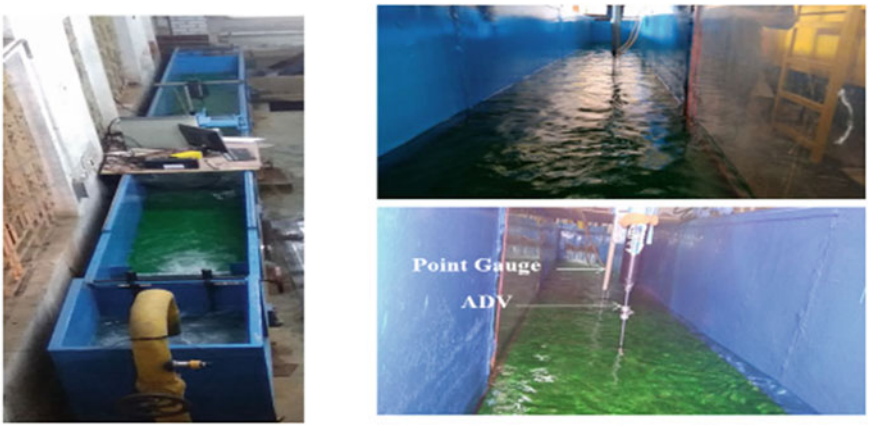

Fig. 12.2 Photographs of experimental set-up, H. E. Lab., NITR

A downstream tail gate is provided to maintain uniformity of flow for this experiment. The tailgate was fixed at a particular height to achieve the given flow depths in steady uniform cases. The same tail gate opening was maintained to achieve the respective flow depths in unsteady flow cases. The measurement of the flow variables has not been done other than the desired flow depth. To get the desired flow depth for the hydrograph, different tail gate settings with several experimental runs have been performed. Rails are provided to support and guide an instrument carriage to run laterally and longitudinally on the top of the flume walls to cover all the test points. The velocity fields were measured by a SonTek Micro 16 MHz Acoustic Doppler velocimeter (ADV). The sampling rate is 50 Hz (the maximum), and the acquisition duration is 60 s. The sampling volume of ADV is located approximately 5 cm below the down-looking probe and was set to be a minimum of 0.09 cm^3. The 5 cm distance between the probe and sampling volume is assumed to minimize the flow interference. ADV can record the three directional velocities U, V, and W in X-direction: along flume bottom, Y-direction: lateral to flume bottom and Z-direction: vertical to flume bottom, respectively. The cross-section distribution of velocities was measured at three different positions or sections (see Fig. 12.1), at $x = 5.5$, 7, and 8.5 m. Then, a Preston tube of outer diameter 4.77 mm was used to measure the velocities at the boundary along the whole perimeter of the flume. The geometry and roughness parameters of the experiment are given in Table 12.1.

The flow behavior at the measuring sections remained similar to that in a long straight natural open channel with a mild bed slope. The ability to reproduce each hydrograph was essential given that only three-point velocities could be observed on each limb during a single run. In the present work, only one hydrograph was studied with successful 198 runs. For maintaining the same flow depth, repetition of the experiments on the same hydrograph has been performed. More runs were taken for the same hydrograph to cover all the measuring points at three different positions for two different flow depths.

Table 12.1 Geometry and roughness parameters for this experiment

Sl no.	Item description	Parameters
1	Channel type	Straight
2	Geometry of channel section	Rectangular
3	Channel base width (b)	0.6 m
4	Depth of channel	0.6 m
5	Bed slope (S_0)	0.0012
6	Length of flume	12 m
7	Length of test channel (X)	10 m
8	Nature of surface bed	Dense rigid grass
9	Flow condition	Unsteady
10	Manning's n of bed material	0.0304

To obtain meaningful and representative values for the mean flow variables, it was fundamental that flow conditions could be consistently repeated, thus minimizing any underlying variability in the unsteady flows. To establish the bulk flow parameters that characterized a hydrograph, estimations were made amid all independent runs for the given hydrograph. The corresponding data for each variable was then ensemble-averaged (i.e., by moving average method) and smoothened. For the steady flows, including the hydrograph base flow, a time of 10 min (600 s) elapsed when a flow was established until the point when measurements were taken or an unsteady flow hydrograph was started. This was guaranteed that flows were fully developed and in equilibrium condition. In each hydrograph run, two same depths of flow have been selected in each for rising and falling cases. For each depth of flow in rising or falling cases, measurements are performed at three positions. Substantial differences between these profiles for the same flow depth in rising and falling cases are observed. Two turbulence characteristics, i.e., mean kinetic energy and turbulent kinetic energy will be calculated and analyzed for the same flow conditions. The variations of these two turbulent characteristics along the three given sections have been demonstrated (Khuntia et al. 2018a, 2019, 2020).

12.3 Results and Discussions

A total of 198 hydrographs was investigated during the experimental repetition. The flow and depth hydrograph in an unsteady flow run has shown in Fig. 12.3. The hysteresis effect of stage-discharge ($h \sim Q$) rating curve between rising and falling limbs is illustrated in Fig. 12.4.

To study the hydrograph, one skewness parameter $\eta = T_r/T_f$ was proposed by Wang et al. (1997), where T_r and T_f are the duration of time for rising and falling limbs. This shape parameter represents hydrograph asymmetry. Based on this definition, one asymmetric hydrograph with the peak skewed toward the rising limb (i.e., η

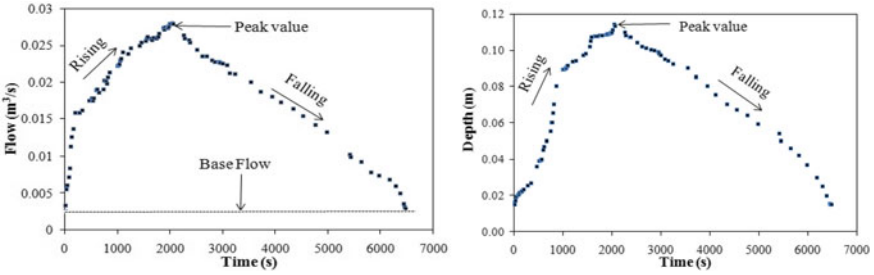

Fig. 12.3 Flow and depth hydrograph in an unsteady flow run

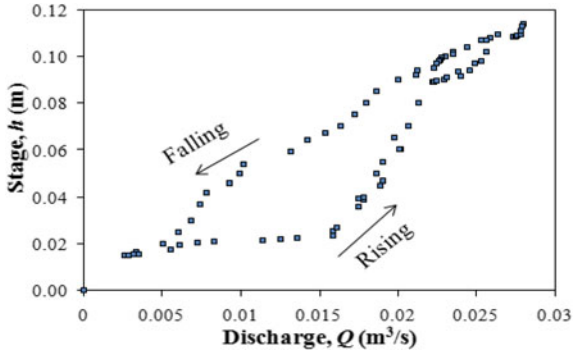

Fig. 12.4 Hysteresis effect in stage-discharge curve

= 0.46, referred to as 'skew-rising' or 'left-skewed' hydrograph) was observed over rigid grass bed (Fig. 12.3). The range of hydraulic parameters used in the experimental run of the hydrograph is given in Table 12.2.

After analyzing the variation of depth-averaged velocity and bed shear stress of a dense rigid rough bed for both steady and unsteady flow conditions, a comparison

Table 12.2 The range of hydraulic parameters used in the experimental runs

Particulars	Value
Slope	0.0012
No of test runs	198
Base flow (m^3/s)	0.0025
Water depth in base flow	0.015 m
Water depth at peak	0.114 m
Time duration for rising limb (T_r)	2040s
Time duration for falling limb (T_f)	4440 s
Total duration of Hydrograph (T)	6480 s
Range of Reynolds's number	400–26,970
Range of Froude number	0.10–0.42

of these flow variables has been made for both the rising and falling limb cases for a given flow depth. Before analyzing the ADV data, possible spectral analysis has been done. The measured data were despiked by an algorithm based on the acceleration thresholding strategy (Goring and Nikora 2002; Khuntia et al. 2018b), which was fit for recognizing and substituting spikes in two stages. The threshold values (=1–1.5) for despiking were determined by trial and error basis, for which the velocity power spectra gave an acceptable fit to the Kolmogorov –5/3 scaling-law in the inertial subrange.

12.3.1 Reynolds Shear Stress Distributions

In addition to the mean velocity, vegetation also affects the turbulence intensity and the diffusion. These turbulence intensities affect the roughness coefficients and also responsible for generating Reynolds stress within stem areas. The Reynolds stress is defined as the time-averaged instantaneous velocity fluctuation in one direction multiplied by the coincident instantaneous velocity fluctuation in another direction. In vegetative flows, there is the possibility of turbulence occurrence due to the vegetation type and density of vegetation. For open channel flow the respective instantaneous velocity fluctuation components, i.e., u', v', and w' in longitudinal, transverse, and vertical directions were calculated to determine the Reynolds stress components, i.e., $\overline{u'v'}$, $\overline{u'w'}$, and $\overline{v'w'}$. The turbulence characteristics can be evaluated by the instantaneous Reynolds stress value for each Reynolds stress plane over the sampling period. The Reynolds stress for all three planes is seen to be substantially higher for the test with vegetation (Dorcheh 2007). The three Reynolds stresses are calculated as per the following equations:

$$\overline{u'v'} = \frac{\sum u' \times v'}{N_T}, \quad \overline{u'w'} = \frac{\sum u' \times w'}{N_T}, \quad \overline{v'w'} = \frac{\sum v' \times w'}{N_T} \tag{12.1}$$

where N_T is total number of data taken at a single point. In the present study, all the three Reynolds stresses (i.e., $\overline{u'v'}$ or $\rho u'v'$, $\overline{v'w'}$ or $\rho v'w'$ and $\overline{u'w'}$ or $\rho u'w'$) along the vertical direction of the channel have been observed and analyzed which are shown in Figs. 12.5, 12.6, and 12.7.

In the beginning section ($x1/X = 0.55$), Reynolds stress component ($\rho u'v'$) is higher as compared to the other two components of Reynolds stress (i.e., $\rho v'w'$ and $\rho u'w'$). In lower flow depth cases, the magnitude of Reynolds stress is less as compared to higher flow depth cases. Also, all three turbulent components reduce their magnitude gradually toward the surface of the water. In falling limbs, the magnitude of $\rho u'v'$ is also higher than that of two other Reynolds stresses (i.e., $\rho v'w'$ and $\rho u'w'$). But, in both rising and falling limb cases, Reynolds stresses are decreasing toward the free surface of the flow depth. The range of Reynolds stresses has varied from -15 to 5 N/m^2 but in the only case of falling limb and higher flow depth case,

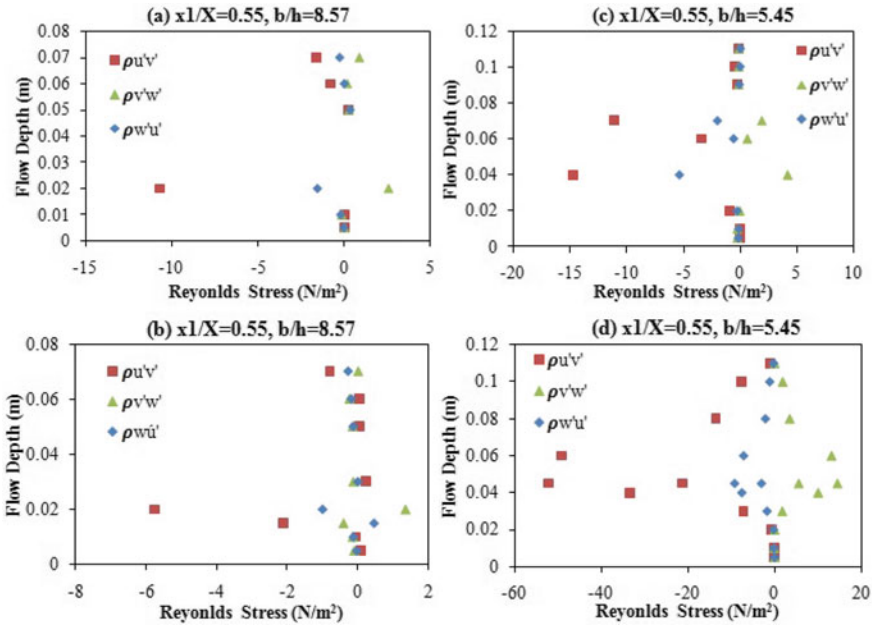

Fig. 12.5 Vertical variation of Reynolds shear stress at section 1 ($x1/X = 0.55$), **a** and **c** rising limb, **b** and **d** falling limb, respectively

and it varies from −55 to 20 N/m^2. More fluctuations that occur in higher flow depth due to more inertia force cause high turbulence in this section. This is because of unsteadiness that causes all the fluctuating velocities u', v′, and w'.

In intermediate section, at section 2 (i.e., $x2/X = 0.70$) in the rising limb, more fluctuations in three Reynolds stresses have been observed in the lower flow depth case, but the higher magnitude in the case of $\rho u'v'$ only. But, in the rising limb case of higher flow depth fluctuation in Reynolds stresses are less as compared to the other three conditions (i.e., Fig. 12.8a, b and d). This may be due to that when the depth of flow for unsteady flow increases more fluctuating of velocity is expected to occur near the side walls due to local friction as well as turbulence due to unsteadiness. This is because of unsteadiness that causes all the fluctuating velocities u', v′, and w'. The range of Reynolds stresses has varied from −7 to 1 N/m^2. In falling limbs, the variations of $\rho u'v'$ and $\rho u'w'$ are more than the magnitude of $\rho v'w'$. The range of Reynolds stresses varied from −2.4 to 0.7 N/m^2.

When moving toward the downstream section ($x3/X = 0.85$), in rising limb case the magnitude of $\rho u'v'$ more as compared to the other two components of Reynolds stress (i.e., $\rho v'w'$ and $\rho u'w'$). The same variation was observed in this section as in Section 1 ($x1/X = 0.55$) except in the case of falling limb in lower flow depth case. This may be due to that, when the flow approached toward downstream section less fluctuating of velocity are expected to occur due to less effect of local friction as well as turbulence due to unsteadiness. In falling limb, the more fluctuation observed in

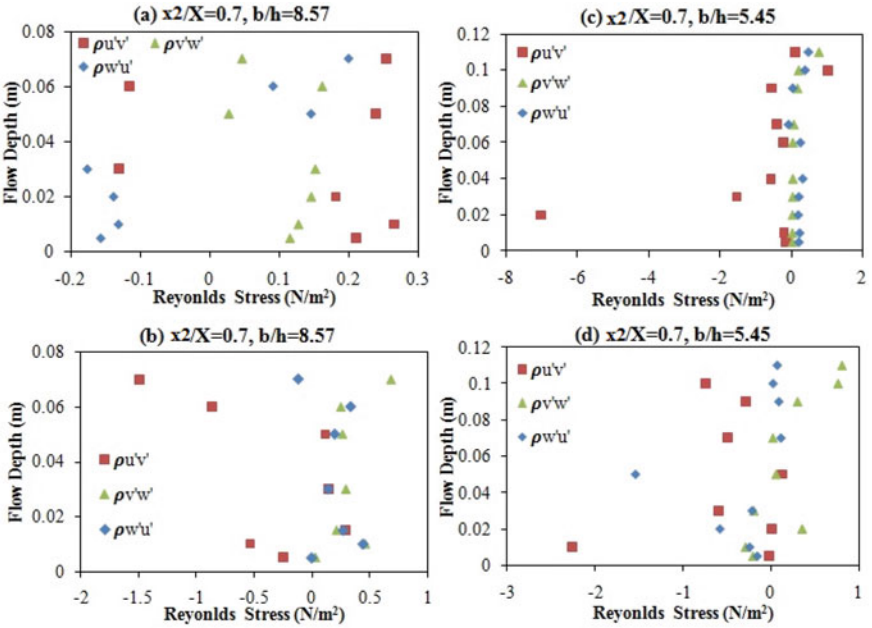

Fig. 12.6 Vertical variation of Reynolds shear stress at section 2 ($x2/X = 0.70$), **a** and **c** rising limb, **b** and **d** falling limb, respectively

Reynolds stresses in the case of lower flow depth as compared to the higher flow depth. The range of Reynolds stresses varied from -6 to 1.8 N/m^2 in the case of rising limb. But, in case of falling limb in low flow depth case, the range varied from -0.4 to 0.3 N/m^2 and in high flow depth case varied from -55 to 18 N/m^2.

Also, in the present research work, all the three Reynolds stresses (i.e., $\overline{u'v'}$ or ρu'v',$\overline{v'w'}$ or $\rho v'w'$ and $\overline{u'w'}$ or $\rho u'w'$) along the lateral direction of the channel have been observed and analyzed which are shown in Figs. 12.8, 12.9, and 12.10.

Interesting results are obtained in all the Reynolds stresses (i.e., $\rho u'$v', ρv'w', and $\rho u'w'$) except for some locations. In rising limb, at lower depth of flow, the higher magnitude of $\rho u'$v' (acting in the vertical plane along the flow direction) is found near the central region of the channel as compared to Reynolds stress in the other two directions (i.e., ρv'w' and $\rho u'w'$). Toward the wall, the Reynolds stress value is found to be same at the beginning of the sections (Section 1, $x1/X = 0.55$). This is because of unsteadiness causes all the fluctuating velocities u', v', and w'. This indicates that the fluctuating of velocity in all directions is found to be same except the central region. At the central region higher fluctuating of longitudinal velocity causes higher magnitude of $\rho u'$v'. When the flow reaches toward the downstream Section 2, ($x2/X = 0.70$), the higher magnitude of ρu'v' are found to be more uniform. Gradually, the Reynolds stress (ρu'v') falls in the central region while rising towards both the walls of the last Section 3 ($x3/X = 0.85$), indicating the fluctuation of turbulence is higher near the walls. For higher depth of flow, the nature of Reynolds stress is found to be

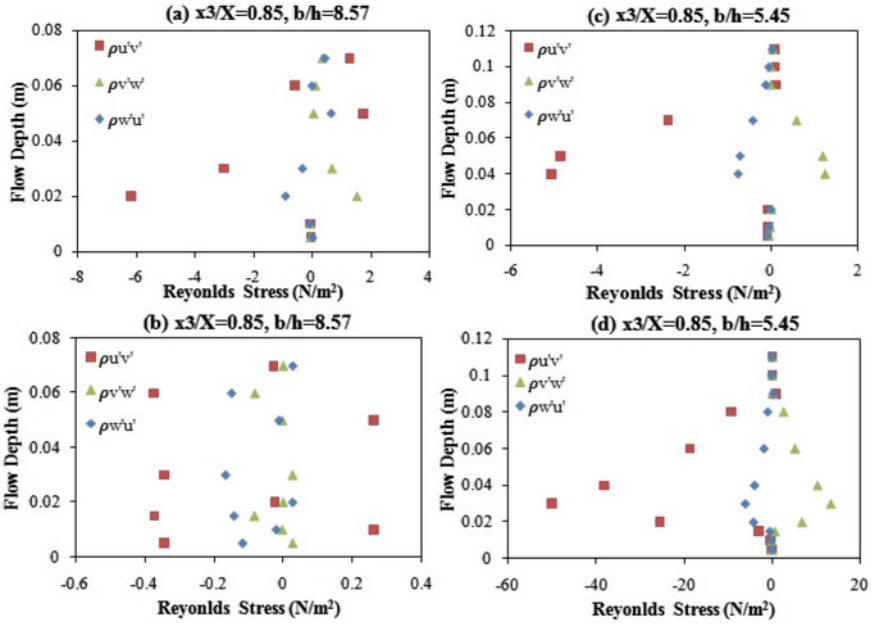

Fig. 12.7 Vertical variation of Reynolds shear stress at section 3 ($x3/X = 0.85$), **a** and **c** rising limb, **b** and **d** falling limb, respectively

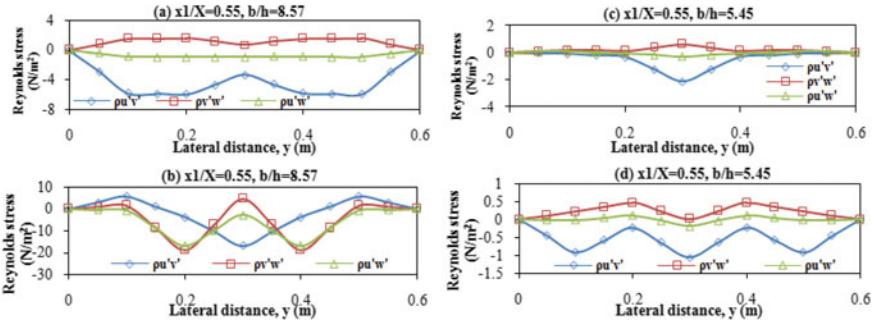

Fig. 12.8 Lateral variation of Reynolds shear stress at section 1 ($x1/X = 0.55$), **a** and **c** rising limb, **b** and **d** falling limb, respectively

in opposite nature that had happened in low depth of flow cases. Here, in Section 1, the higher value of $\rho u'v'$ are found to be near the wall regions, whereas in Section 3 the higher magnitude of $\rho u'v'$ are found in the central regions. This may be due to that when the depth of flow for unsteady flow increases more fluctuating of velocity are expected to occur near the side walls due to local friction as well as turbulence due to unsteadiness.

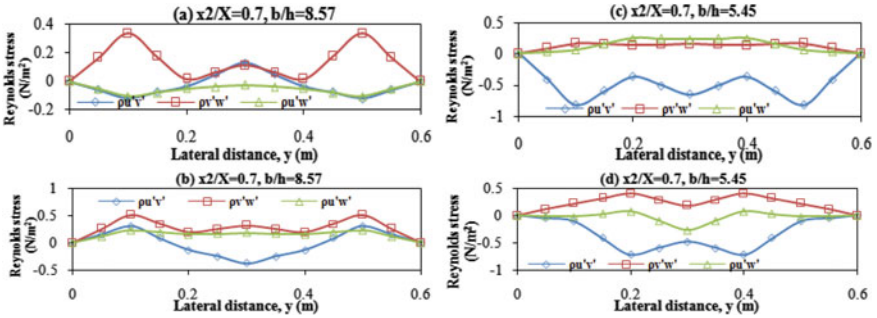

Fig. 12.9 Lateral variation of Reynolds shear stress at section 2 ($x2/X = 0.70$), **a** and **c** rising limb, **b** and **d** falling limb, respectively

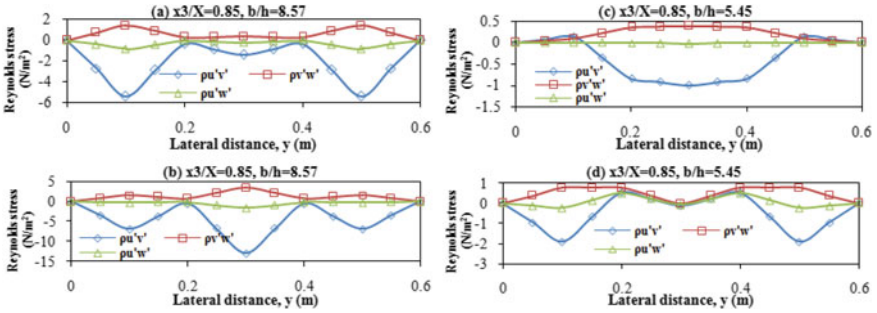

Fig. 12.10 Lateral variation of Reynolds shear stress at section 3 ($x3/X = 0.85$), **a** and **c** rising limb, **b** and **d** falling limb, respectively

In the case of falling limb, all the Reynolds stresses are of lesser magnitude in the range ± 0.5 N/m^2. At Section 1, Reynolds stress ($\rho u'v'$) value is found to be maximum in the central region of the channel. But the other two Reynolds stresses (i.e., $\rho v'w'$ and $\rho u'w'$) are having two peak values at the middle third regions and least value of the central region. In Section 2, the peak values of $\rho u'v'$ is found in the central region. There is a peak drop of $\rho u'v'$ is noticed in the central region of the channel. Similarly, in Section 3, there is a sudden drop in $\rho u'$v$'$ is noticed, but with a high magnitude in range (± 15 N/m^2). For higher depth of flow, the range of Reynolds stress value is less as compared to that of the low depth of flow. At Section 1, there are three peaks of $\rho u'v'$ is noticed which occurred in the central region and two middle third points. At Sections 2 and 3, the central peak diminishes and only two peaks lie at two middle third points. As compared to lower depth of flow in high flow depth, the range of Reynolds stress is of smaller magnitude (± 2 N/m^2). In lower depth of flow, the range of Reynolds stress is ± 20 N/m^2, this is due to the dominating effect of both bottom turbulence and bed friction.

12.4 Conclusions

The following concluding remarks have been drawn from this study:

1. An experiment has been conducted to investigate the turbulence characteristics in terms of Reynolds stress variation under unsteady flow conditions in a rough open channel for two different flow depths each in rising and falling limbs of hydrograph.
2. In the case of lower flow depth and rising limb, the magnitude of Reynolds stress is less as compared to higher flow depth cases. Also, all the three turbulent components reduce their magnitude gradually toward the surface of the water.
3. In rising limb, more fluctuations in three Reynolds stresses have been observed in the lower flow depth case, but the higher magnitude in case of $\rho u'v'$ only. But, in the rising limb case of higher flow depth fluctuation in Reynolds stresses are less as compared to the other three conditions (i.e., Fig. 12.8a, b and d).
4. At the downstream sections, in the rising limb case the magnitude of $\rho u'v'$ more as compared to the other two components of Reynolds stress (i.e., $\rho v'w'$ and $\rho u'w'$). In falling limbs, more fluctuation was observed in Reynolds stresses in the case of lower flow depth as compared to the higher flow depth.
5. In the rising limb, for lower depth of flow near the wall region, the magnitude of Reynolds stress value is higher as compare to that of the higher depth of flow. But in the case of falling limb at higher depth of flow, less magnitude of Reynolds stresses have been observed as compared to the lower depth of flow.
6. The present study is a direct measurement of turbulence characteristics. So, this may help to solve any turbulence models (i.e., Spalart–Allmaras (S-A) model, $k-\varepsilon$ model, $k-\omega$ model, and Menter's Shear Stress Transport (SST) model etc.), especially in unsteady flow conditions.

References

Ahanger MA, Asawa GL, Lone MA (2008) Experimental study of sediment transport hysteresis. J Hydraul Res 46(5):628–635

Anwar HO, Atkins R (1980) Turbulence measurements in simulated tidal flow. J Hydraul Div 106(8):1273–1289

Bombar G, Elçi Ş, Tayfur G, Güney MŞ, Bor A (2011) Experimental and numerical investigation of bed-load transport under unsteady flows. J Hydraul Eng 137(10):1276–1282

De Sutter R, Huygens M, Verhoeven R (1970) Unsteady open channel flow registrations in a test flume with circular cross-section. WIT Trans Model Simul 17

De Sutter R, Verhoeven R, Krein A (2001) Simulation of sediment transport during flood events: laboratory work and field experiments. Hydrol Sci J 46(4):599–610

Dorcheh SAM (2007) Effect of rigid vegetation on the velocity, turbulence, and wave structure in open channel flows. Doctoral dissertation, Cardiff University, UK

Dupuis V, Proust S, Berni C, Paquier A (2017) Compound channel flow with a longitudinal transition in hydraulic roughness over the floodplains. Environ Fluid Mech 1–26

Goring DG, Nikora VI (2002) Despiking acoustic Doppler velocimeter data. J Hydraul Eng 128(1):117–126

Hu J, Yang S, Fu X (2012) Experimental investigation on propagating characteristics of sinusoidal unsteady flow in open-channel with smooth bed. Sci China Technol Sci 1–11

Huai W, Hu Y, Zeng Y, Han J (2012) Velocity distribution for open channel flows with suspended vegetation. Adv Water Resourc 49:56–61

Khuntia JR, Devi K, Proust S, Khatua KK (2018a) Depth-averaged velocity and bed shear stress in unsteady open channel flow over rough bed. In: River Flow 2018, E3S web of conferences, vol 40, p 05071

Khuntia JR, Devi K, Khatua KK (2018b) Prediction of depth-averaged velocity in an open channel flow. Appl Water Sci. Springer 8(6):1–14

Khuntia JR, Devi K, Khatua KK (2019) Turbulence characteristics in a rough open channel under unsteady flow conditions. ISH J Hydraulic Eng 1–12

Khuntia JR, Proust S, Khatua KK (2020) Unsteady open-channel flows over rough bed with and without emergent rigid vegetation: A laboratory experiment. In: River Flow 2020. CRC Press, Taylor & Francis, pp 1527–1535

Mahmood K, Yevjevich V (eds) (1975) Unsteady flow in open channels, vol 1. Water Resource Publisher, Fort Collins, Colo

Martin RL, Jerolmack DJ (2013) Origin of hysteresis in bed form response to unsteady flows. Water Resour Res 49(3):1314–1333

Nezu I, Kadota A, Nakagawa H (1994a) Experimental study on turbulent structures in unsteady open-channel flows. In: Proceedings of the symposium on fundamentals and advancements 1n hydraulic measurements and experimentation, ASCE, Buffalo, New York, pp 185–193

Nezu I, Nakagawa H, Jirka GH (1994) Turbulence in open-channel flows. J Hydraulic Eng 120(10):1235–1237

Song TC, Graf WH (1996) Velocity and turbulence distribution in unsteady open-channel flows. J Hydraul Eng 122(3):141–154

Tu H, Graf WH (1992) Vertical distribution of shear stress in unsteady open-channel flow [hydrographs were investigated in a gravel-bed flume]. In: Proceedings of the institution of civil engineers: water maritime and energy, vol 96, pp 63–69

Velasco D, Bateman A, Redondo JM, DeMedina V (2003) An open channel flow experimental and theoretical study of resistance and turbulent characterization over flexible vegetated linings. Flow Turbul Combust 70(1):69–88

Wang Z, Lin B, Nestmann F (1997) Prospects and new problems of sediment research. Int J Sediment Res 12(1):1–5